Dalton Transactions

ROYAL SOCIETY OF CHEMISTRY

PERSPECTIVE

View Article Online
View Journal | View Issue

Cite this: *Dalton Trans.*, 2026, **55**, 4763

Rational design and applications of artificial metalloenzymes based on neuroglobin

Li-Juan Sun[a] and Ying-Wu Lin *[b]

The rational design of artificial metalloenzymes enables the expansion of the functionalities of natural metalloenzymes, which has become a research hotspot in biocatalysis. As a member of the globin family, neuroglobin (Ngb) has a stable structure and possesses a tunable intramolecular disulfide bond of Cys46–Cys55, making it an ideal protein scaffold for the rational design of artificial metalloenzymes. This article systematically reviews the recent progress in the rational design and applications of artificial metalloenzymes based on Ngb. It highlights strategies such as optimizing the microenvironment in the heme center, substituting key amino acid residues, constructing additional intramolecular disulfide bonds, and introducing metal cofactors such as Co-porphyrin, which have successfully endowed Ngb-based artificial metalloenzymes with functions including nitrite reductase, monooxygenase, peroxidase, carbene transferase, hydrogenase, and even carbon monoxide detoxification capabilities. These advances not only deepen the understanding of the structure–function relationships of heme enzymes but also provide new insights into the rational design of artificial metalloenzymes. Artificial metalloenzymes based on Ngb and other protein scaffolds are expected to play significant roles in areas such as green synthesis, biocatalysis, environmental remediation, biomedicine, *etc*.

Received 10th January 2026,
Accepted 30th January 2026

DOI: 10.1039/d6dt00067c

rsc.li/dalton

Introduction

Metalloenzymes are a crucial class of enzymes whose activity relies mainly on metal ions or metal complexes as cofactors, such as the heme prosthetic group.[1] These enzymes perform vital catalytic functions in biological systems, including redox reactions, hydrolysis, disproportionation, isomerization, *etc*. However, natural metalloenzymes have inherent limitations. For example, their stability often decreases at high temperatures or in organic solvents, which hinders their direct application in many industrial processes.[2]

As alternatives to natural metalloenzymes, artificial metalloenzymes (ArMs), which are constructed by integrating metal catalysts with biomacromolecules such as proteins or nucleic

[a]*Chongqing Youth Vocational & Technical College, Chongqing 400712, China*
[b]*School of Chemistry and Chemical Engineering, University of South China, Hengyang 421001, China. E-mail: ywlin@usc.edu.cn*

Li-Juan Sun

Li-Juan Sun received her PhD from the University of South China in 2024 under the supervision of Prof. Ying-Wu Lin, and joined Chongqing Youth Vocational & Technical College in 2025. Her research focuses on the design of functional metalloenzymes based on Mb and Ngb, and she has published six peer-reviewed papers.

Ying-Wu Lin

Ying-Wu Lin is a full professor at the University of South China. He received his PhD from Fudan University in 2005 and conducted postdoctoral research at the University of Illinois Urbana-Champaign (2018–2010) with Prof. Yi Lu. In 2013, he received a JSPS fellowship with Prof. Shun Hirota at the Nara Institute of Science and Technology. Currently, his group focuses on the structure and function of metalloenzymes, as well as the design of artificial metalloenzymes based on heme proteins for potential applications.

acids to form superior catalytic systems, have attracted widespread attention over the past decades.[3] Generally, engineered enzymes based on natural proteins but endowed with artificial functions might also be considered within the scope of ArMs. Heme-containing enzymes are a major class of metalloenzymes, such as horseradish peroxidase (HRP) and cytochrome P450.[4] Considerable studies have been devoted to the design of ArMs with new functions based on heme proteins. For instance, ArMs constructed using myoglobin (Mb) and cytochrome P450 scaffolds have been used for the catalytic oxidation and reduction of various substrates, as well as for non-natural reactions such as carbene transfer reactions.[5–8]

Neuroglobin (Ngb) belongs to the globin family, along with hemoglobin (Hb) and Mb. Since its first discovery in the vertebrate brains in 2000,[9] Ngb has received significant attention due to its unique structure and potential biological functions (Fig. 1). Unlike Hb and Mb, which primarily function as oxygen carriers, Ngb typically forms a bis-His (His64/His96) heme coordination.[10] Furthermore, the presence of a disulfide bond between Cys46 and Cys55 in human Ngb modulates the coordination behavior of His64, thereby regulating the binding of small molecules such as O_2, CO, and NO to the heme iron.[11,12] These distinctive structural features suggest possible roles of Ngb in electron transfer and in the regulation of reactive oxygen/nitrogen species (ROS/RNS).[13]

Recent advances in the fields of protein engineering and computation-aided protein design have rendered Ngb an ideal protein scaffold for the construction of ArMs (Fig. 1). The rational design of ArMs containing a heme cofactor typically involves the modulation of the microenvironment of the heme active center to confer new catalytic functions.[14,15] Such approaches may include substituting key residues, modifying substrate-binding pockets, and introducing unnatural amino acids or non-native metal cofactors. For instance, mutating the heme axial ligand His64 in Ngb disrupts its native bis-His coordination, creating an open heme site for catalysis.[16] These modifications enable Ngb to mimic the structural features of natural heme enzymes such as peroxidases and P450s, resulting in functional conversions.[17]

Currently, Ngb-based ArMs exhibit excellent performance, thus representing important case studies for the rational design of ArMs. This article reviews the recent progress in the rational design of Ngb-based ArMs. It focuses on the structural basis of Ngb as a protein scaffold, and strategies for optimizing the heme active center and expanding catalytic functions. We also discuss the potential applications of Ngb-based ArMs in biocatalysis, green synthesis and environmental remediation. The aim is to provide structural information and technical guidance for the development of an efficient, sustainable next generation of biocatalysts.

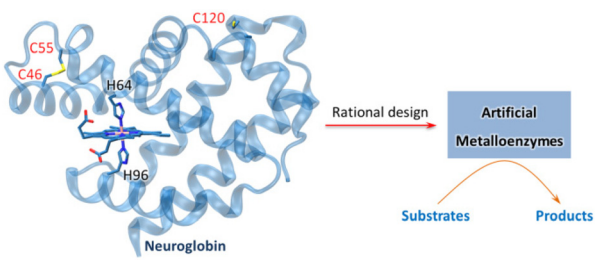

Fig. 1 X-ray crystal structure of human neuroglobin (PDB code 4MPM)[10] and the design of artificial metalloenzymes.

Rational design and applications

Artificial nitrite reductase

The nitrogen cycle is one of the most important biogeochemical cycles on Earth. It encompasses processes such as nitrogen fixation (the conversion of atmospheric nitrogen to ammonia), nitrification (the oxidation of ammonia to nitrate), and denitrification (the reduction of nitrate to N_2).[18] Nitrite reductase (NIR) is a key enzyme in denitrification that is widely present in organisms, and catalyzes the reduction of nitrite (NO_2^-) to NO under hypoxic or anaerobic conditions.[19] In addition to their normal physiological functions, various heme proteins (*e.g.*, Hb, Mb, and Ngb) may also exhibit some NIR activity under hypoxic conditions.[20] Studies have shown that this activity depends largely on the structural features of the heme active center. Rational protein design can effectively modulate its catalytic efficiency, providing important insights for developing ArMs with NIR activity.

In 2005, Gladwin and coworkers discovered that the O_2 carrier Hb exhibits NIR function during the transition from oxygenated (Relaxed-state, R-state) to deoxygeneated (Tense-state, T-state) states, catalyzing the reduction of NO_2^- to NO, with the catalytic rate regulated by the R- and T-state equilibrium of the Hb tetramer.[21] Shiva *et al.*[22] also found that deoxy Mb shows NIR activity, generating NO and regulating mitochondrial respiration. Studies on Mb-knockout mice by Hendgen-Cotta *et al.*[23] revealed that Mb can directly catalyze the reduction of NO_2^- to NO, thereby inhibiting cellular respiration, limiting ROS production and reducing oxidative damage to prevent myocardial infarction. In previous studies, we optimized the heme center of Mb by constructing a double mutant of F43H/H64A Mb with a suitable distal histidine located at position 43 and a water channel to the heme center, which increased the NIR catalytic efficiency by ~8-fold.[24] Furthermore, this ArM could be employed to modulate the concentration of RNS in breast cancer cells, thereby inducing apoptosis.[25]

As a member of the globin family, Ngb has a similar 3D-structure to Hb and Mb. Meanwhile, it has a unique intramolecular disulfide bond Cys46–Cys55 (Fig. 1), which is a distinctive feature of Ngb-based artificial NIRs. Tiso *et al.*[26] discovered that the redox state of this disulfide bond controls the coordination state of the heme center (Fig. 2A), thereby modulating its NIR activity. Disulfide bond formation increased NIR catalytic activity by approximately 2-fold (catalytic efficiency: 0.12 *vs.* 0.062 M^{-1} s^{-1}). Tejero *et al.*[27] systematically investigated the NIR catalytic mechanism of Ngb using site-directed

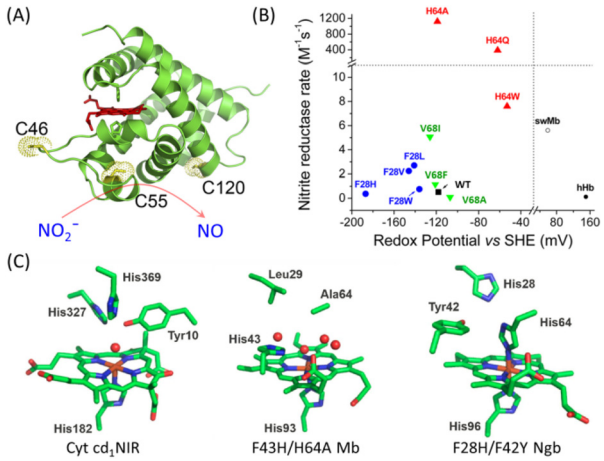

Fig. 2 Design of artificial NIR based on Ngb: (A) a model structure of Ngb with the disulfide bond of C46–C55 in a reduced state and the catalysis of nitrite to nitric oxide, reproduced from ref. 26; (B) the relationship between the redox potential and NIR rate for Ngb and its mutants, with Hb and Mb shown for comparison, reproduced from ref. 27; (C) the X-ray structures of Cyt cd_1 NIR and the designed F43H/H64A Mb, and the model structure of F28H/F42Y Ngb, reproduced from ref. 29.

mutagenesis to modify amino acids in the heme cavity, such as Phe28, His64, and Val68. The general difference between Ngb and Hb/Mb is that Hb and Mb have a six-coordinated heme center (H_2O/His) and exhibit higher redox potentials than Ngb with a bis-His coordination. The nitrite reduction rate of Ngb was found to correlate weakly with its redox potential; instead, it is primarily governed by the accessibility of the heme distal site, with mutations at the His64 site showing the most significant impact (Fig. 2B). Notably, H64A Ngb exhibited a remarkably high catalytic rate of 1120 M^{-1} s^{-1}, representing the fastest artificial NIRs reported to date and suggesting potential future applications. Meanwhile, the H64A Mb mutant exhibits NIR activity only one-third that of WT Mb (5.6 M^{-1} s^{-1}),[24] suggesting that other structural features of the heme active site may be responsible for the high NIR activity of H64A Ngb.

Inspired by the structural features of cytochrome cd_1-type nitrite reductase (*e.g.*, a distal His and Tyr in the heme center)[28] and the protein design based on Mb from our group (F43H/H64A Mb featuring a distal His and a water channel),[24] Tejero *et al.*[29] hypothesized that introducing F28H and F42Y mutations in Ngb might mimic the heme micro-environments and potentially enhance NIR activity (Fig. 2C). However, experimental results showed that single mutants F28H and F42Y, and the double mutant F28H/F42Y did not improve the NIR catalytic rate of Ngb; instead, showed decreased activities. This may be attributed to differences in the steric constraints for the heme cavity, the dynamic property of the key residues (*e.g.*, His64), and the redox potentials compared to those of natural enzymes and Mb-based artificial NIRs. This study highlights that the unique structural and dynamic features of the protein scaffold must be considered in the rational design of ArMs.

Artificial monooxygenases

Monooxygenases (*e.g.*, cytochrome P450) are important oxidases that activate O_2 at the heme center to form highly reactive oxidative species (*e.g.*, Fe(IV)=O$^{\bullet+}$).[30] These intermediates can insert a single oxygen atom into substrates, enabling crucial reactions such as hydroxylation and epoxidation.[4] These enzymes have broad applications in green biosynthesis and in the research area of pharmaceuticals. Significant attention has been paid to the investigation of the structure–function relationship of these enzymes, as well as to the design of artificial monooxygenases.

During our investigation of the Ngb structure and function, we found that replacing the heme axial ligand His64 with methionine resulted in the H64M Ngb mutant in a high-spin heme state, which suggests that Met64 did not coordinate with the heme.[31] High-resolution mass spectrometry revealed that Met64 underwent self-oxidation to methionine sulfoxide (SO-Met) and sulfone (SO_2-Met) (Fig. 3A), while other Met residues and Cys120 remained unmodified. This phenomenon resembles the self-oxidation behavior of Met80 in cytochrome *c* (Cyt *c*) under non-native states.[32] Mechanism studies suggest that Met64, located at the heme distal site, may undergo oxidation involving O_2 activation, similar to the catalytic mechanism of Cyt P450,[30] implying monooxygenase-like functionality.

To further probe the self-oxidation function of H64M Ngb, we rationally constructed V71C Ngb and H64M/V71C Ngb mutants by introducing a Cys residue close to the heme 4-vinyl group (Fig. 3B), inspired by previous studies on heme proteins, Cyt b_5 and Cyt b_{562}.[33,34] The H64M/V71C Ngb mutant was found to form a single thioether bond (Cys71-heme 4-vinyl). Mass spectrometry further confirmed the oxidation of Met64 to the sulfone form (SO_2-Met), a modification similar to the non-native state of Cyt *c* under oxidative stress.[32] However, the single mutant V71C Ngb retained bis-His coordination and did not form the thioether bond, as confirmed by the crystal struc-

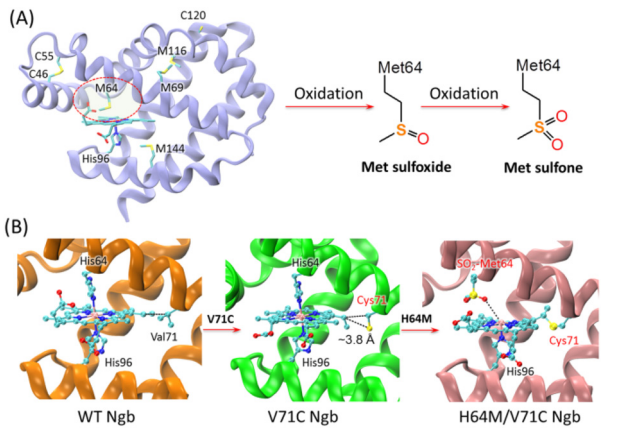

Fig. 3 (A) H64M Ngb with monooxygenase activity catalyzing the self-oxidation of Met64; (B) design of Cyt *c*-like C–S bonds based on Ngb, with the X-ray crystal structures of WT Ngb and V71C Ngb, and model structure of H64M/V71C Ngb shown for comparison, reproduced from ref. 35.

ture of V71C Ngb (PDB code 8GRZ).[35] This finding indicates that an open distal site is essential for generating active intermediates of the heme iron, inducing post-translational modifications.

Subsequent studies showed that thioether bond formation significantly enhanced protein stability. The midpoint (C_m) of guanidine hydrochloride (Gdn·HCl)-induced protein denaturation increased by ~0.24 M, and the temperature of thermally induced denaturation increased by over 20 °C. Furthermore, this mutant exhibited an accelerated rate of forming the active species upon reaction with the oxidant *meta*-chloroperoxybenzoic acid (*m*-CPBA), suggesting higher reactivity in oxidative catalysis. Further investigations are required to test other substrates, such as those contain a sulfur group, for oxidation. The findings demonstrate the potential of protein engineering to construct P450-like artificial monooxygenases based on Ngb. In addition, they provide significant insights into the structure–function regulation of heme proteins in non-native states.

Artificial peroxidase

Heme-containing peroxidases are widespread in nature, typically using H_2O_2 or organic peroxides (*e.g.*, *m*-CPBA) as electron acceptors to catalyze the oxidation of various substrates. They play crucial roles in key physiological processes like oxidative stress defense and immune responses.[36] Common representatives include HRP and myeloperoxidase (MPO).[4] Due to their high catalytic efficiency and strong substrate specificity, they are widely used in biosensing and biocatalysis. In recent decades, rational design and practical applications of artificial peroxidases have advanced significantly, by modifying either natural proteins (*e.g.*, Mb, Cyt *c*) or *de novo* designed protein scaffolds.[37] Moreover, recent progress has been made in engineering P450 peroxidases from their monooxygenase modes.[38,39] Typically, these engineered P450 peroxidases can catalyze new reactions such as the nitration of unsaturated hydrocarbons and the one-electron oxidation of aromatic amines.[40,41]

Ngb contains three Cys residues, with Cys46 and Cys55 forming a disulfide bond within the protein (Fig. 1). However, the surface-exposed Cys120 often leads to purification difficulties, reduced stability, and dimer formation.[42,43] To overcome these problems, common methods often replace Cys120 with serine.[44] We used a different method by rationally designing a new intramolecular disulfide bond to protect Cys120 while further enhancing the protein stability. Based on structural analysis and prediction of Ngb, we introduced Cys at position 15, spatially proximal to Cys120, to construct a Cys15–Cys120 disulfide bond. The crystal structure of the A15C mutant (PDB code 7VQG)[45] confirmed that this mutant retained the native C46–C55 disulfide bond and formed the designed C15–C120 disulfide bond (Fig. 4A). Structural analysis also revealed cavities near the heme center capable of binding small organic molecules, suggesting multifunctional possibilities. Furthermore, thermal stability assays showed that this mutant has a very high unfolding temperature (T_m > 100 °C).[46]

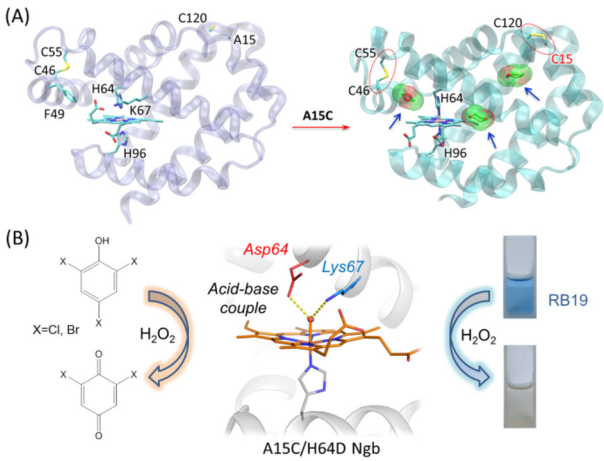

Fig. 4 (A) Rational design of A15C Ngb with double disulfide bonds based on Ngb (PDB code 7VQG); (B) artificial peroxidase A15C/H64D Ngb designed based on A15C Ngb catalyzing the dehalogenation and dye-decolorization reactions, reproduced from ref. 16 with permission from American Chemical Society, Copyright 2021.

Given the excellent expression yield and thermal stability of A15C Ngb, we constructed the A15C/H64D double mutant. The design was inspired by native chloroperoxidase (CPO), which contains a crucial distal Asp in its heme active site.[47] The double mutations successfully convert Ngb into a highly efficient multifunctional peroxidase.[16] The introduction of an aspartate (Asp64) at the heme center, together with the naturally occurring lysine 67 (Lys67), forms an "Asp64-Lys67" acid–base catalytic pair (Fig. 4B), which significantly enhances its ability to activate H_2O_2 to form catalytic species. This ArM exhibited excellent dehaloperoxidase activity, with catalytic efficiencies for 2,4,6-trichlorophenol (TCP) and 2,4,6-tribromophenol (TBP) approximately 50-fold and 78-fold higher than that of the native dehaloperoxidase (DHP), respectively, and even about 3-fold higher than that of HRP. This study demonstrates the possibility of designing efficient artificial peroxidases based on Ngb, and also provides new insights for developing multifunctional biocatalysts for environmental remediation, such as for the degradation of halophenols and treatment of wastewater containing organic dyes.

Based on this progress, we further introduced Tyr49 near the heme through rational design to facilitate electron transfer, a process crucial for the oxidation of organic substrates that has been previously shown.[48] The constructed triple mutant A15C/H64D/F49Y Ngb efficiently catalyzed the synthesis of indigo and its derivatives (Fig. 5A).[49] Using H_2O_2 as the oxidant without expensive cofactors, the catalytic efficiency of this mutant for indigo synthesis (714 M^{-1} s^{-1}) was significantly higher than those of previously reported Mb mutants (~2–4 fold)[50] and even surpassed some Cyt P450 mutants.[51] Furthermore, this enzyme efficiently catalyzed the coupling oxidation of indole derivatives containing –Cl, –Br, and –NO_2 substituents to produce indigo derivatives with various colors, with yields up to ~90% and chemoselectivity up to ~97%. The

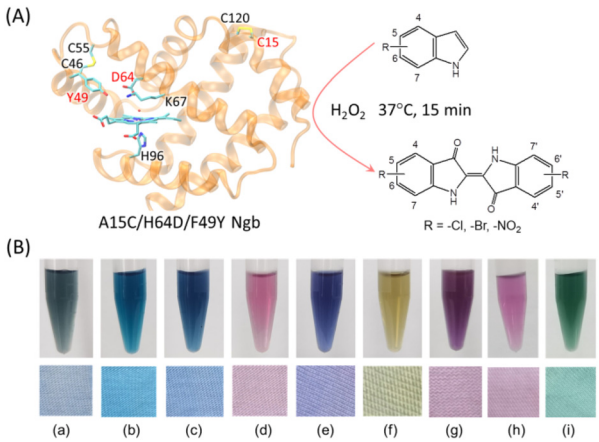

Fig. 5 (A) Model structure of A15C/H64D/F49Y Ngb and catalysis of indole to form indigo and derivatives; (B) the solutions of indigo and its derivatives, and their effects on dyeing: (a) indigo, (b) 4,4′-dichloroindigo, (c) 5,5′-dichloroindigo, (d) 6,6′-dichloroindigo, (e) 7,7′-dichloroindigo, (f) 4,4′-dinitroindigo, (g) 5,5′-dinitroindigo, (h) 6,6′-dibromoindigo, and (i) 4-chloroindole/4-nitroindole (n : n = 2 : 1).

synthesized dyes could be used for dyeing cotton, yielding uniform colors including blue, red, yellow, purple, and even green (Fig. 5B). Therefore, these ArMs have potential for use in the dyeing industry.

Artificial carbene transferases

Artificial carbene transferases are non-natural biocatalysts obtained through protein engineering (including directed evolution) of natural heme proteins (*e.g.*, P450 enzymes and Mb) or *de novo* designed proteins (*e.g.*, 4-helix bundles).[52] They can efficiently and selectively catalyze carbene transfer reactions, including highly enantioselective cyclopropanation, inert C–H bond insertion, and N–H, B–H, and Si–H bond insertions.[8] These enzymes enable transformations difficult to achieve with traditional chemical catalysts and expand the functionalities of biocatalysis, which provide powerful and sustainable tools for green synthesis and the preparation of intermediates for pharmaceuticals.

Inspired by the study of Prof. Frances Arnold's group,[53] and in an effort to further expand the functionalities of A15C Ngb-based ArMs for new reactions such as carbene transfer, we screened key amino acid residues around its heme center (*e.g.*, Phe42 and Val68). Among a series of mutants, the double mutant A15C/H64G Ngb exhibited excellent performance in catalyzing carbene N–H insertion reactions with aromatic amine derivatives. It efficiently catalyzed the N–H insertion reaction between ethyl diazoacetate (EDA) and aniline substrates, with yields up to >99% and total turnover numbers (TTN) up to 33 000.[54] This represents one of the highest reported values, approximately 110-fold higher than those initially reported based on Cyt P450.[53] Moreover, the enzyme tolerated various substituents (both electron-donating and electron-withdrawing) and even catalyzed reactions with bulky substrates like 1-aminopyrene.

Furthermore, this ArM was found to catalyze two successive N–H insertions with *o*-phenylenediamine derivatives, followed by cyclization to form quinoxalinone products (Fig. 6A), as confirmed by X-ray crystallography. This represents the first reported example of an ArM catalyzing such cyclization. A proposed catalytic mechanism is shown in Fig. 6B. First, EDA reacts with the reduced protein to form a carbene intermediate, which then undergoes two N–H insertions with *o*-phenylenediamine. The product undergoes spontaneous cyclization at room temperature or upon heating, followed by dehydrogenation in air to yield the final quinoxalinone products. This study not only expands the application of the Ngb scaffold in the catalysis of non-natural reactions but also provides a novel biocatalyst for the efficient synthesis of bioactive molecules (*e.g.*, amino acid derivatives and nitrogen-containing heterocycles).

Given the important biological activities of boron-containing compounds,[55,56] we further designed and optimized artificial carbene transferases based on A15C Ngb for catalyzing asymmetric B–H insertion reactions to synthesize chiral organoboron compounds.[57] Through computer-aided rational design, we identified the highly active quadruple mutant A15C/H64G/V68F/F28M Ngb (Fig. 7A). It efficiently catalyzed the asymmetric B–H insertion reaction between pyridine/quinoline boranes and benzyl 2-diazopropanoate (BnDP) and its derivatives (docking results are shown in Fig. 7B), achieving products with enantiomeric ratios up to 98 : 2 (crystal structure confirmed the *R*-configuration, Fig. 7C). The designed heme distal cavity could also accommodate bulky substrates, such as those containing quinoline, naphthyl, or biphenyl groups. Furthermore, whole cells or cell lysates containing this enzyme effectively catalyzed the reaction. This work represents the first development of Ngb as a biocatalytic platform for synthesizing

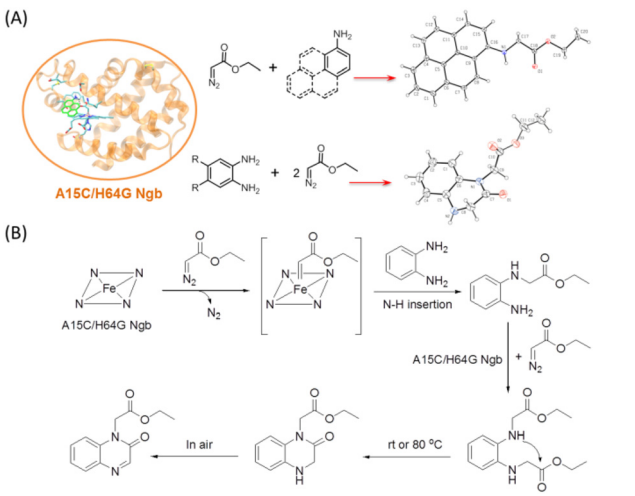

Fig. 6 Design of artificial carbene transferase based on Ngb for catalyzing N–H insertion reaction: (A) artificial metalloenzyme A15C/H64G Ngb catalyzing single or double N–H insertion reactions between ethyl diazoacetate and aniline substrates and (B) the proposed mechanism of the double N–H insertion reaction catalyzed by A15C/H64G Ngb with *o*-phenylenediamine to form quinoxalinone products.

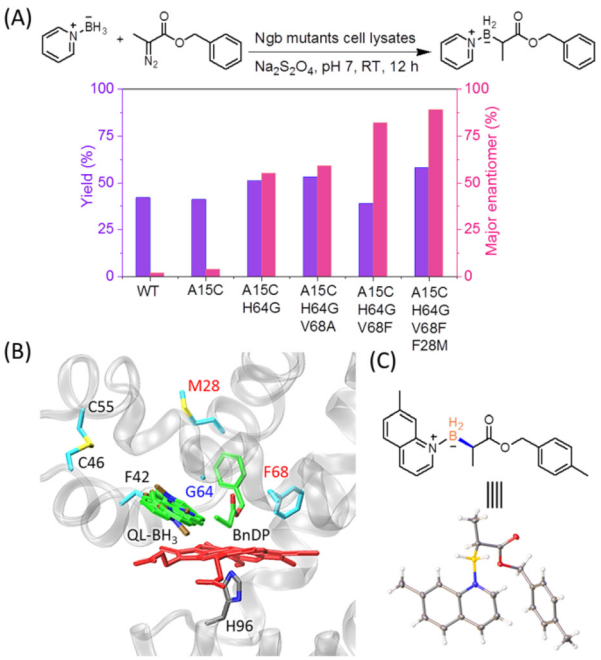

Fig. 7 Design of artificial carbene transferase based on Ngb for catalyzing B–H insertion reaction: (A) yields and major enantiomer of the B–H insertion product of pyridine-borane with BnDP catalyzed by cell lysates of Ngb and its mutants; (B) docking structures of A15C/H64G/V68F/F28M Ngb upon the binding of BnDP and quinolone-borane (QL-BH3); (C) the chemical and X-ray structure of the product, reproduced from ref. 57 with permission from American Chemical Society, Copyright 2024.

chiral organoboron compounds, which expands the application of heme proteins in asymmetric synthesis, providing a new route for the efficient and green preparation of bioactive chiral organoborons.

Artificial hydrogenases

Hydrogenases are metalloenzymes that catalyze the reversible oxidation of H_2 or the reduction of H^+ to H_2, widely found in microorganisms. Their active centers typically contain iron, nickel, or other metal atoms, such as in [NiFe]- and [FeFe]-type hydrogenases.[58,59] Artificial hydrogenases are biocatalysts constructed through rational design or modification of natural proteins to mimic the catalytic function of natural hydrogenases, enabling efficient and tunable H_2 production. These artificial enzymes are often designed based on stable protein scaffolds (*e.g.*, Mb and Cyt *c*) by introducing or optimizing active centers (*e.g.*, incorporating iron, nickel, or cobalt ions or their complexes) to confer hydrogenase activity.[60–62] For example, Sommer *et al.* chose Mb as the scaffold and reconstituted cobalt porphyrin (Co-PP) into apo-Mb.[63] Electrochemical studies showed that the resulting CoPP-Mb exhibited significant catalytic current for H^+ reduction in aqueous solution. Under photochemical conditions (1 mM $[Ru(bpy)_3]^{2+}$, pH 7), it produced H_2 with a turnover number (TON) of 518 over 12 h.

Using a similar approach for heme substitution with Co-PP, Meglioli *et al.* constructed CoPP-Ngb and its disulfide-deficient mutant CoPP-C46A/C55A Ngb.[64] The electrochemical and spectroscopic properties were studied and the potential as bioelectrocatalysts for H_2 production were evaluated. They found that in both CoPP-bound proteins, the cobalt metal was in a six-coordinate low-spin state, presumably with bis-His (His64/His96) axial coordination, and the electrochemical properties were largely unaffected by the absence of the disulfide bond. CoPP substitution was found to significantly lower the reduction potential of the metal center compared to that of the heme-bound Ngb, which also eliminated the rotation phenomenon of the heme group as observed in Ngb. Furthermore, when CoPP-Ngb and CoPP-C46A/C55A Ngb were immobilized on a pyrolytic graphite electrode, both enzymes effectively catalyzed the reduction of H^+ to H_2 near neutral pH (Fig. 8). Although their catalytic efficiency was slightly lower than that of 6-coordinate (H_2O/His93) CoPP-Mb, CoPP-Ngb exhibited greater tolerance to the presence of O_2, offering a new system for developing biomimetic catalysts capable of operating under aerobic conditions. These results also reveal the specificity in the regulation of the structure and function of CoPP-substituted heme proteins, and lay an important foundation for future design of artificial hydrogenases by exploring the strategy of metal cofactor substitution.

Artificial carbon monoxide antidote

Carbon monoxide (CO) poisoning is one of the most common forms of poisoning worldwide, primarily caused by incomplete combustion of carbon-containing materials.[65] CO has an extremely high affinity for Hb, approximately 200 times that of O_2, rapidly forming carboxyhemoglobin (CO-Hb), which impedes oxygen transport, leading to tissue hypoxia (Fig. 9A).[66] Additionally, CO can bind to various heme proteins (*e.g.*, Mb and Ngb), interfering with cellular metabolism, inducing ROS accumulation, and causing cellular damage. Currently, the primary treatment for CO poisoning is oxygen therapy, including hyperbaric oxygen, but it has limitations such as limited facilities and contraindications, making it difficult to meet all clinical needs. Therefore, developing novel antidotes is of great significance.[65,66]

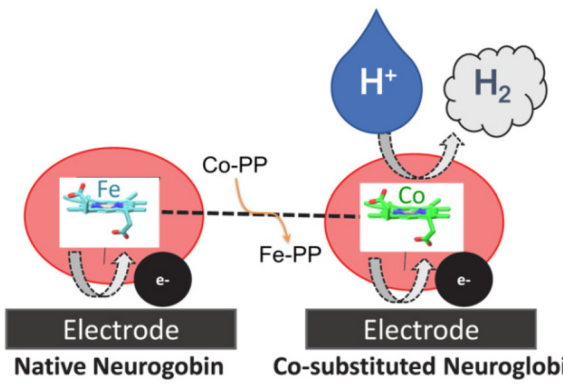

Fig. 8 Design of artificial hydrogenase Co-PP-Ngb based on Ngb and the catalysis of H_2 production on an electrode, reproduced from ref. 64.

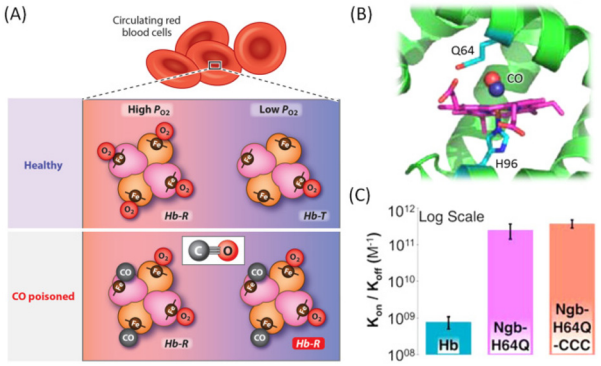

Fig. 9 Design of the CO antidote based on Ngb: (A) CO binding to the heme site of Hb in blood cells and diminishing O_2 carrying capacity, reproduced from ref. 66; (B) a model of CO binding to the heme site of Ngb-H64Q; and (C) comparison of CO binding affinity, reproduced from ref. 67 with permission from ASBMB, Copyright 2020.

Gladwin's group found that mutating the distal His64 of Ngb to glutamine (H64Q) converted the heme iron from a bis-His 6-coordinate state to a mono-His 5-coordinate state.[67] The resulting Ngb-H64Q mutant exhibited a very high CO binding affinity (Fig. 9B). Subsequently, they further mutated the three cysteine residues in Ngb and constructed a triple mutant (C46G/C55S/C120S, termed Ngb-H64Q-CCC) to enhance biocompatibility. Spectroscopic studies showed that this mutant possessed high CO binding rates and low oxidation rates, with a CO affinity (K_{on}/K_{off}) approximately 320 times that of Hb (Fig. 9C), and could rapidly capture CO under aerobic conditions. *In vitro* experiments confirmed that this mutant significantly accelerated CO dissociation from free Hb and red blood cells. In a mouse model of CO poisoning, it effectively restored the heart rate and blood pressure and improved survival. Furthermore, the CO-Ngb-H64Q-CCC complex was rapidly excreted *via* the kidneys, demonstrating good safety.

In a follow-up study, Gladwin *et al.*[68] further investigated the role of Ngb-H64Q-CCC in mitigating CO-induced mitochondrial toxicity. They found that CO not only binds to Hb but also inhibits functions like that of mitochondrial cytochrome *c* oxidase (C*c*O). In a lethal CO poisoning mouse model, Ngb-H64Q-CCC not only restored respiratory function in cardiac tissue but also repaired the activity of complexes I, II, and IV in the electron transport chain. *In vitro* mitochondrial experiments further demonstrated that this mutant could not only scavenge CO from the blood but also reverse the inhibitory effect of CO on the mitochondrial respiratory chain, thereby improving oxygen utilization and energy metabolism in tissues. Therefore, protein engineering based on Ngb shows promise as a novel therapeutic agent for the future clinical treatment of CO poisoning. It should be noted that although repurposed Ngb-H64Q-CCC may not be classified as an artificial heme enzyme, its novel functionality offers a distinct detoxification strategy, complementing the current standard of care dominated by oxygen therapy.

Conclusion and perspectives

The design and application of artificial metalloenzymes are a popular area of research in biocatalysis. This review provides a systematic summary of the recent progress in the rational design of ArMs, focusing on the use of Ngb as a protein scaffold. Ngb exhibits characteristics such as structural stability and high expression yield. It also has a tunable intramolecular disulfide bond (Cys46–Cys55) and potential substrate-binding sites, making it an ideal platform for constructing multifunctional ArMs. Through rational design strategies, such as optimizing the heme microenvironment and substituting metal cofactors, Ngb has been successfully transformed into ArMs with high catalytic activity. These ArMs can perform functions such as those of NIR, monooxygenase, peroxidase, carbene transferase and hydrogenase. They also demonstrate potential as a CO antidote. These studies deepen our understanding of the structure–function relationship of heme proteins and demonstrate the potential of protein engineering to expand biocatalytic functions.

Nevertheless, research on Ngb-based ArMs is still in a developmental stage, with requirements for improvement in catalytic efficiency, substrate scope, and practical applications. For instance, the combination of time-resolved spectroscopy and theoretical calculations has the potential to elucidate the structures of key intermediate states during catalysis by Ngb-based ArMs.[69] A comprehensive understanding of catalytic mechanisms can serve as a theoretical foundation for further functional optimization. Alongside rational design, machine learning (*e.g.*, tools like ProteinMPNN)[70] could be used to predict and optimize protein structures, which can enhance enzyme stability under extreme conditions (*e.g.*, organic solvents, high temperature, and non-physiological pH) and help to efficiently design active centers and substrate binding sites, thereby moving from "rational design" to "intelligent design". Furthermore, there is a need to further explore the potential of Ngb-based ArMs in biosynthesis, biosensing, and bioenergy.

In conclusion, with the deepening integration of protein engineering, synthetic biology, and computational chemistry, ArMs based on Ngb and other protein scaffolds (*e.g.*, Mb, P450, Cyt c, and *de novo* designed proteins) are expected to move from basic research to practical applications, playing important roles in green synthesis, biocatalysis, environmental remediation, biomedicine, *etc.*

Conflicts of interest

There are no conflicts to declare.

Data availability

No primary research results, software or code have been included and no new data were generated or analysed as part of this review.

Acknowledgements

The research on ArM design based on Ngb from our group was supported by the National Natural Science Foundation of China (32171270 and 21977042).

References

1 J. Liu, S. Chakraborty, P. Hosseinzadeh, Y. Yu, S. Tian, I. Petrik, A. Bhagi and Y. Lu, *Chem. Rev.*, 2014, **114**, 4366–4469.
2 R. Buller, S. Lutz, R. J. Kazlauskas, R. Snajdrova, J. C. Moore and U. T. Bornscheuer, *Science*, 2023, **382**, eadh8615.
3 T. Vornholt, F. Leiss-Maier, W. J. Jeong, C. Zeymer, W. J. Song, G. Roelfes and T. R. Ward, *Nat. Rev. Methods Primers*, 2024, **4**, 78.
4 T. L. Poulos, *Chem. Rev.*, 2014, **114**, 3919–3962.
5 K. Oohora and T. Hayashi, *Dalton Trans.*, 2021, **50**, 1940–1949.
6 O. F. Brandenberg, K. Chen and F. H. Arnold, *J. Am. Chem. Soc.*, 2019, **141**, 8989–8995.
7 A. L. Chandgude and R. Fasan, *Angew. Chem., Int. Ed.*, 2018, **57**, 15852–15856.
8 Y. Yang and F. H. Arnold, *Acc. Chem. Res.*, 2021, **54**, 1209–1225.
9 T. Burmester, B. Weich, S. Reinhardt and T. Hankeln, *Nature*, 2000, **407**, 520–523.
10 B. G. Guimaraes, D. Hamdane, C. Lechauve, M. C. Marden and B. Golinelli-Pimpaneau, *Acta Crystallogr., Sect. D:Biol. Crystallogr.*, 2014, **70**, 1005–1014.
11 J. T. Trent 3rd, R. A. Watts and M. S. Hargrove, *J. Biol. Chem.*, 2001, **276**, 30106–30110.
12 M. Bellei, C. A. Bortolotti, G. Di Rocco, M. Borsari, L. Lancellotti, A. Ranieri, M. Sola and G. Battistuzzi, *J. Inorg. Biochem.*, 2018, **178**, 70–86.
13 P. Ascenzi, A. di Masi, L. Leboffe, M. Fiocchetti, M. T. Nuzzo, M. Brunori and M. Marino, *Mol. Aspects Med.*, 2016, **52**, 1–48.
14 F. Nastri, M. Chino, O. Maglio, A. Bhagi-Damodaran, Y. Lu and A. Lombardi, *Chem. Soc. Rev.*, 2016, **45**, 5020–5054.
15 Y.-W. Lin, *Coord. Chem. Rev.*, 2017, **336**, 1–27.
16 S.-F. Chen, X.-C. Liu, J.-K. Xu, L. Li, J.-J. Lang, G.-B. Wen and Y.-W. Lin, *Inorg. Chem.*, 2021, **60**, 2839–2845.
17 S. Fan and Z. Cong, *Acc. Chem. Res.*, 2024, **57**, 613–624.
18 W. G. Zumft, *Microbiol. Mol. Biol. Rev.*, 1997, **61**, 533–616.
19 D. Nurizzo, M. C. Silvestrini, M. Mathieu, F. Cutruzzola, D. Bourgeois, V. Fulop, J. Hajdu, M. Brunori, M. Tegoni and C. Cambillau, *Structure*, 1997, **5**, 1157–1171.
20 M. T. Gladwin and D. B. Kim-Shapiro, *Blood*, 2008, **112**, 2636–2647.
21 Z. Huang, S. Shiva, D. B. Kim-Shapiro, R. P. Patel, L. A. Ringwood, C. E. Irby, K. T. Huang, C. Ho, N. Hogg, A. N. Schechter and M. T. Gladwin, *J. Clin. Invest.*, 2005, **115**, 2099–2107.
22 S. Shiva, Z. Huang, R. Grubina, J. Sun, L. A. Ringwood, P. H. MacArthur, X. Xu, E. Murphy, V. M. Darley-Usmar and M. T. Gladwin, *Circ. Res.*, 2007, **100**, 654–661.
23 U. B. Hendgen-Cotta, M. W. Merx, S. Shiva, J. Schmitz, S. Becher, J. P. Klare, H. J. Steinhoff, A. Goedecke, J. Schrader, M. T. Gladwin, M. Kelm and T. Rassaf, *Proc. Natl. Acad. Sci. U. S. A.*, 2008, **105**, 10256–10261.
24 L. B. Wu, H. Yuan, S. Q. Gao, Y. You, C. M. Nie, G. B. Wen, Y. W. Lin and X. Tan, *Nitric Oxide*, 2016, **57**, 21–29.
25 X.-Y. Tong, X.-Z. Yang, X. Teng, S.-Q. Gao, G.-B. Wen and Y.-W. Lin, *Arch. Biochem. Biophys.*, 2022, **730**, 109399.
26 M. Tiso, J. Tejero, S. Basu, I. Azarov, X. Wang, V. Simplaceanu, S. Frizzell, T. Jayaraman, L. Geary, C. Shapiro, C. Ho, S. Shiva, D. B. Kim-Shapiro and M. T. Gladwin, *J. Biol. Chem.*, 2011, **286**, 18277–18289.
27 J. Tejero, C. E. Sparacino-Watkins, V. Ragireddy, S. Frizzell and M. T. Gladwin, *Biochemistry*, 2015, **54**, 722–733.
28 M. R. Cheesman, S. J. Ferguson, J. W. Moir, D. J. Richardson, W. G. Zumft and A. J. Thomson, *Biochemistry*, 1997, **36**, 16267–16276.
29 M. D. Williams, V. Ragireddy, M. R. Dent and J. Tejero, *Biochem. Biophys. Rep.*, 2023, **36**, 101560.
30 I. Shin, Y. Wang and A. Liu, *Proc. Natl. Acad. Sci. U. S. A.*, 2021, **118**, e2106561118.
31 H.-X. Liu, L. Li, B. He, S.-Q. Gao, G.-B. Wen and Y.-W. Lin, *Dalton Trans.*, 2018, **47**, 10847–10852.
32 Z. Wang, Y. Ando, A. D. Nugraheni, C. Ren, S. Nagao and S. Hirota, *Mol. BioSyst.*, 2014, **10**, 3130–3137.
33 Y.-W. Lin, W.-H. Wang, Q. Zhang, H.-J. Lu, P.-Y. Yang, Y. Xie, Z.-X. Huang and H.-M. Wu, *ChemBioChem*, 2005, **6**, 1356–1359.
34 P. D. Barker, E. P. Nerou, S. M. V. Freund and I. M. Fearnley, *Biochemistry*, 1995, **34**, 15191–15203.
35 L. Chen, H. Yuan, X.-J. Wang, L. Li, X. Tan and Y.-W. Lin, *ChemBioChem*, 2022, **23**, e202200531.
36 Y. Yi, P. Jia, P. Xie, X. Peng, X. Zhu, S. Yin, Y. Luo, Y. Deng and L. Wan, *Front. Immunol.*, 2025, **16**, 1683876.
37 F. Nastri, D. D'Alonzo, L. Leone, G. Zambrano, V. Pavone and A. Lombardi, *Trends Biochem. Sci.*, 2019, **44**, 1022–1040.
38 N. Ma, W. Fang, C. Liu, X. Qin, X. Wang, L. Jin, B. Wang and Z. Cong, *ACS Catal.*, 2021, **11**, 8449–8455.
39 F. Jiang, Z. Wang and Z. Cong, *Faraday Discuss.*, 2024, **252**, 52–68.
40 X. Wang, X. Lin, Y. Jiang, X. Qin, N. Ma, F. Yao, S. Dong, C. Liu, Y. Feng, L. Jin, M. Xian and Z. Cong, *Angew. Chem., Int. Ed.*, 2023, **62**, e202217678.
41 J. Chen, F. Yao, Y. Jiang, X. Qin, M. Xian, Y. Feng and Z. Cong, *Adv. Sci.*, 2025, **12**, 2412100.
42 G. Di Rocco, F. Bernini, G. Battistuzzi, A. Ranieri, C. A. Bortolotti, M. Borsari and M. Sola, *FEBS J.*, 2023, **290**, 148–161.
43 A. Cassiani, P. G. Furtmüller, M. Borsari, G. Battistuzzi and S. Hofbauer, *Biosci. Rep.*, 2025, **45**, 1–13.
44 A. Bocahut, V. Derrien, S. Bernad, P. Sebban, S. Sacquin-Mora, E. Guittet and E. Lescop, *J. Biol. Inorg. Chem.*, 2013, **18**, 111–122.

45 S. Q. Gao, H. Yuan, X. C. Liu, L. Li, X. Tan, G. B. Wen and Y. W. Lin, *Proteins*, 2022, **90**, 1152–1158.
46 H.-X. Liu, L. Li, X.-Z. Yang, C.-W. Wei, H.-M. Cheng, S.-Q. Gao, G.-B. Wen and Y.-W. Lin, *RSC Adv.*, 2019, **9**, 4172–4179.
47 M. Sundaramoorthy, J. Terner and T. L. Poulos, *Structure*, 1995, **3**, 1367–1377.
48 M. J. Field, R. K. Bains and J. J. Warren, *Dalton Trans.*, 2017, **46**, 11078–11083.
49 L. Chen, J.-K. Xu, L. Li, S.-Q. Gao, G.-B. Wen and Y.-W. Lin, *Mol. Syst. Des. Eng.*, 2022, **2022**, 239–247.
50 J. Xu, O. Shoji, T. Fujishiro, T. Ohki, T. Ueno and Y. Watanabe, *Catal. Sci. Technol.*, 2012, **2**, 739–744.
51 O. Rousseau, M. C. C. J. C. Ebert, D. Quaglia, A. Fendri, A. H. Parisien, J. N. Besna, S. Iyathurai and J. N. Pelletier, *ChemCatChem*, 2020, **12**, 837–845.
52 K. Hou, W. Huang, M. Qi, T. H. Tugwell, T. M. Alturaifi, Y. Chen, X. Zhang, L. Lu, S. I. Mann, P. Liu, Y. Yang and W. F. DeGrado, *Science*, 2025, **388**, 665–670.
53 Z. J. Wang, N. E. Peck, H. Renata and F. H. Arnold, *Chem. Sci.*, 2014, **5**, 598–601.
54 L.-J. Sun, H. Wang, J.-K. Xu, S.-Q. Gao, G.-B. Wen and Y.-W. Lin, *Inorg. Chem.*, 2023, **62**, 16294–16298.
55 S. B. J. Kan, X. Huang, Y. Gumulya, K. Chen and F. H. Arnold, *Nature*, 2017, **552**, 132–136.
56 R. J. Grams, W. L. Santos, I. R. Scorei, A. Abad-García, C. A. Rosenblum, A. Bita, H. Cerecetto, C. Viñas and M. A. Soriano-Ursúa, *Chem. Rev.*, 2024, **124**, 2441–2511.
57 L. J. Sun, H. Wang, J. K. Xu, W. Niu, S. Q. Gao and Y. W. Lin, *Org. Lett.*, 2024, **26**, 8872–8877.
58 X. Brazzolotto, J. K. Rubach, J. Gaillard, S. Gambarelli, M. Atta and M. Fontecave, *J. Biol. Chem.*, 2006, **281**, 769–774.
59 H. Tai and S. Hirota, *ChemBioChem*, 2020, **21**, 1573–1581.
60 D. J. Sommer, M. D. Vaughn, B. C. Clark, J. Tomlin, A. Roy and G. Ghirlanda, *Biochim. Biophys. Acta*, 2016, **1857**, 598–603.
61 D. Selvan, P. Prasad, E. R. Farquhar, Y. Shi, S. Crane, Y. Zhang and S. Chakraborty, *ACS Catal.*, 2019, **9**, 5847–5859.
62 A. E. Wertz, P. Teptarakulkarn, R. E. Stein, P. J. Moore and H. S. Shafaat, *Biochemistry*, 2023, **62**, 2622–2631.
63 D. J. Sommer, M. D. Vaughn and G. Ghirlanda, *Chem. Commun.*, 2014, **50**, 15852–15855.
64 M. Meglioli, F. Sebastiani, M. Bellei, G. Di Rocco, A. Ranieri, C. A. Bortolotti, M. Sola, M. Borsari, G. Smulevich and G. Battistuzzi, *Inorg. Chem.*, 2025, **64**, 9066–9083.
65 A. L. Parker and T. C. Johnstone, *J. Inorg. Biochem.*, 2024, **251**, 112453.
66 M. R. Dent, J. J. Rose, J. Tejero and M. T. Gladwin, *Annu. Rev. Med.*, 2024, **75**, 337–351.
67 I. Azarov, L. Wang, J. J. Rose, Q. Xu, X. N. Huang, A. Belanger, Y. Wang, L. Guo, C. Liu, K. B. Ucer, C. F. McTiernan, C. P. O'Donnell, S. Shiva, J. Tejero, D. B. Kim-Shapiro and M. T. Gladwin, *Sci. Transl. Med.*, 2016, **8**, 368ra173.
68 J. J. Rose, K. A. Bocian, Q. Xu, L. Wang, A. W. DeMartino, X. Chen, C. G. Corey, D. A. Guimarães, I. Azarov, X. N. Huang, Q. Tong, L. Guo, M. Nouraie, C. F. McTiernan, C. P. O'Donnell, J. Tejero, S. Shiva and M. T. Gladwin, *J. Biol. Chem.*, 2020, **295**, 6357–6371.
69 V. Modi and Y. Zhang, *Chem. Commun.*, 2025, **61**, 15789–15805.
70 K. H. Sumida, R. Núñez-Franco, I. Kalvet, S. J. Pellock, B. I. M. Wicky, L. F. Milles, J. Dauparas, J. Wang, Y. Kipnis, N. Jameson, A. Kang, J. De La Cruz, B. Sankaran, A. K. Bera, G. Jiménez-Osés and D. Baker, *J. Am. Chem. Soc.*, 2024, **146**, 2054–2061.